### Title
Correction to “Total Synthesis of (−)-Chromodorolide B By a Computationally-Guided Radical Addition/Cyclization/Fragmentation Cascade”




### Journal
Journal of the American Chemical Society, 141(1)

### ISSN
0002-7863



### Authors
Tao, Daniel J
Slutskyy, Yuriy
Muuronen, Mikko
et al.



### Publication Date
2019-01-09

### DOI
10.1021/jacs.8b13203

Peer reviewed

# Total Synthesis of (-)-Chromodorolide B By a Computationally-Guided Radical Addition/Cyclization/Fragmentation Cascade

Daniel J. Tao, Yuriy Slutskyy, Mikko Muuronen, Alexander Le, Philipp Kohler, and Larry E. Overman*

[†]Department of Chemistry, University of California, Irvine, California 92697-2025

**ABSTRACT:** The first total synthesis of a chromodorolide marine diterpenoid is described. The core of the diterpenoid is constructed by a bimolecular radical addition/cyclization/fragmentation cascade that unites two complex fragments and forms two C-C bonds and four contiguous stereogenic centers of (-)-chromodorolide B in a single step. This coupling step is initiated by visible-light photocatalytic fragmentation of a redox-active ester, which can be accomplished in the presence of an iridium or a less-precious electron-rich dicyanobenzene photocatalyst, and employs equimolar amounts of the two addends. Computational studies guided the development of this central step of the synthesis and provide insight into the origin of the observed stereoselectivity.

## INTRODUCTION

Convergent strategies where advanced fragments of a target molecule are prepared in parallel and joined together at the latest possible stage in a synthesis are nearly always more efficient than linear strategies.[1] A corollary of this fact is the importance of reactions that are capable of combining complex molecules efficiently with high regio- and stereoselectivity. Recent investigations have shown that bimolecular-coupling reactions of tertiary carbon radicals can unite advanced synthetic fragments of structurally complex natural products in an efficient fashion.[2,3] Cascade reactions in which an intermediate produced in a bond-forming reaction propagates to construct additional bonds of a target molecule also typically increase efficiency in a chemical synthesis.[4] Radical cascade reactions, in particular intramolecular radical cascades, have long played a significant role in the efficient construction of complex molecules.[4,5] Much less developed are strategies in which a bimolecular radical coupling reaction initiates a further bond-forming cascade sequence.[6] The discovery of such a stereoselective sequence, whose optimization was guided by computational analysis, led to the first total synthesis of the marine diterpenoid chromodorolide B and is the subject of this article.[7]

## BACKGROUND

The rearranged spongian diterpenoids are a large and structurally diverse family of natural products, which have been isolated largely from marine sources (Figure 1).[8] Distinct members of this group are characterized by the presence of a hydrophobic unit connected by a single bond to a highly oxygenated *cis*-2,8-dioxabicyclo[3.3.0]octan-3-one fragment, as exemplified by dermalactone (**1**),[9] norrisolide (**2**),[10] cheloviolene A (**3**),[11] macfarladin C (**4**),[12] or a 2,7-dioxabicyclo[3.2.1]octan-3-one fragment as found in aplyviolene (**5**),[13] macfarlandin E (**6**),[12] shahamin F (**7**),[14] verrielactone (**8**),[15] and norrlandin (**9**).[16] In chromodorolides A-E (**10**-**14**),[17–19] these bicyclic frameworks are appended to an additional oxygenated cyclopentane ring.

The chromodorolides have been isolated from nudibranchs in the genus *Chromodoris* and from encrusting sponges on which these nudibranchs potentially feed. Chromodorolide A (**10**) was first reported in 1989 by Anderson and Clardy, with its novel structure being revealed by X-ray crystallography.[17a] Two years later these workers described a second diterpenoid found in skin extracts of the tropical dorid nudibranch *Chromodoris cavae*, which showed a high frequency carbonyl stretching band at 1812 $cm^{-1}$ in its IR spectrum.[17b] Detailed analyses of $^{1}H$ and $^{13}C$ NMR spectra indicated that this diterpenoid, chromodorolide B (**11**), had the same chromodorane carbon skeleton as chromodorolide A, but the bridging lactone ring in this case was 5-membered. Analogues of **10** and **11**, chromodorolides C–E (**12**–**14**) that display different degrees of acetylation of the vicinal hydroxyl substituents were isolated subsequently from two different marine sponges.[18,19] The chromodorolides are the most structurally intricate of the spongian diterpenoids, with 10

contiguous stereocenters arrayed upon their pentacyclic ring systems. Prior to the investigations reported in this account, the absolute configuration of the chromodorolides was proposed upon the basis of their presumed biosynthesis from diterpenoids having the spongian ring system.[20]

Modest *in vitro* antitumor, nematocidal and antimicrobial activities have been reported for various chromodorolides.[17b,18,19a] Because of their structural relationship with molecules such as norrisolide (**2**), cheloviolene A (**3**) and macfarlandin E (**6**),[21,22] which have pronounced effects on the Golgi apparatus, the activity of the chromodorolides on the structure and function of the Golgi apparatus is potentially more significant. In our own investigations of analogues harboring 2,7-dioxabicyclo[3.2.1]octan-3-one or *cis*-2,8-dioxabicyclo[3.3.0]octan-3-one fragments, we have identified conjugation of these ring systems with lysine side chains of proteins to form pyrrole adducts as potentially involved in the biological activities of diterpenoids such as those depicted in Figure 1.[22] As a result of the little-studied biological activity of the chromodorolides, and the challenge apparent in assembling these densely functionalized diterpenoids, we initiated studies to develop chemical syntheses of the chromodorolides. In this account, we detail the investigations that led to a concise, stereocontrolled total synthesis of (–)-chromodorolide B (**11**).

**Figure 1**

**A.** Representative structurally diverse rearranged spongian diterpenes that harbor the c

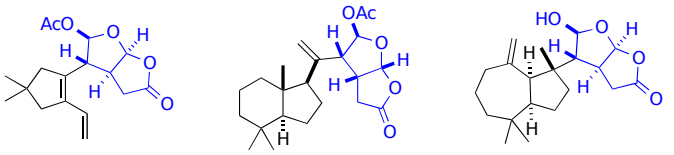

dermalactone (**1**) norrisolide (**2**) cheloviolene A (**3**)

**B.** Representative structurally diverse rearranged spongian diterpenes that harbor the c

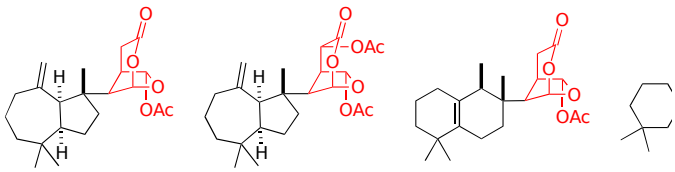

aplyviolene (**5**) macfarlandin E (**6**) shahamin F (**7**) ve

## RESULTS AND DISCUSSION

**General Synthetic Strategy.** Retrosynthetically, we envisioned disconnecting the lactone bonds in **10** and **12** to arrive at a common tetracyclic acid intermediate **15** (Scheme 1). We hypothesized that both bridged and fused tricyclic frameworks could be prepared from acid **15** by site-selective oxocarbenium ion formation, followed by intramolecular lactonization. The *cis*-2,8-dioxabicyclo[3.3.0]octan-3-one fragment of chromodorolide C (**12**) is likely to be accessed most readily, as kinetically favored 5-membered ring closure of **17** could dominate even if oxocarbenium ion formation were unselective yet reversible.[22] In contrast, to construct the 2,7-dioxabicyclo[3.2.1]octan-3-one fragment found in chromodorolide A (**10**) regioselective activation at C-15 would be required to permit less-kinetically favored lactonization of oxocarbenium ion **16**. The successful development of a strategy to form tetracyclic intermediate **15** and its conversion to (–)-chromodorolide B (**11**) is detailed in this report.[7]

**Scheme 1**

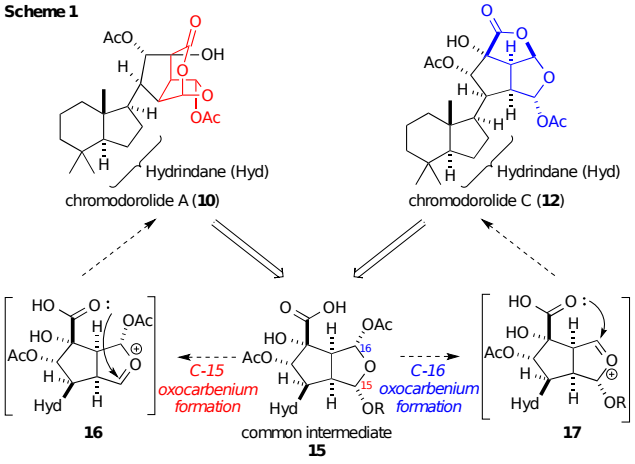


**Early Studies.** Our initial thoughts on accessing the highly oxygenated bicyclic motif found in **15** envisaged late-stage dihydroxylation of an alkene precursor (Scheme 2). We expected that oxidation of an intermediate such as **18** would take place from the convex face opposite the bulky hydrindane fragment to generate **19**. As this step would occur late in the synthesis, we examined this conversion initially in a model

system harboring an isopropyl group in place of the hydrindane fragment.[23] *cis*-Oxabicyclo[3.3.0]octenone **20** was readily assembled from an allenoate precursor by a diastereoselective phosphine-promoted (3+2) annulation.[24] To our surprise, dihydroxylation of **20** took place with high stereoselectivity from the concave face to give mainly diol **21**. Other oxidants such as *m*-chloroperoxybenzoic acid or dimethyldioxirane behaved similarly, giving crystalline epoxide **23** as the predominant product.[25,26a] Computational studies by the Houk group suggested that the contrasteric selectivity for dihydroxylation of the enoate **20** arose from torsional effects.[23,27] Torsional, electrostatic and steric effects can all influence stereoselection in dihydroxylations of *cis*-bicyclo[3.3.0]octenes, and a more general discussion of this issue has been published.[23]

**Scheme 2**

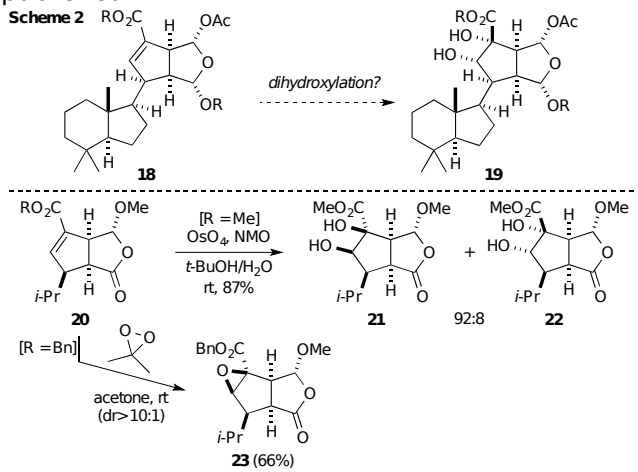


**Revised Synthesis Plan: A Bimolecular Radical Addition/Cyclization/Fragmentation Cascade.** As installation of the *cis*-diol functionality did not appear to be feasible from a *cis*-oxabicyclo[3.3.0]octenone precursor, we turned to a plan wherein the *cis*-diol would be incorporated early in the synthetic sequence (Figure 2A). Disconnection of the lactone ring of chromodorolides A or B series leads to intermediate **24**. Further simplification leads

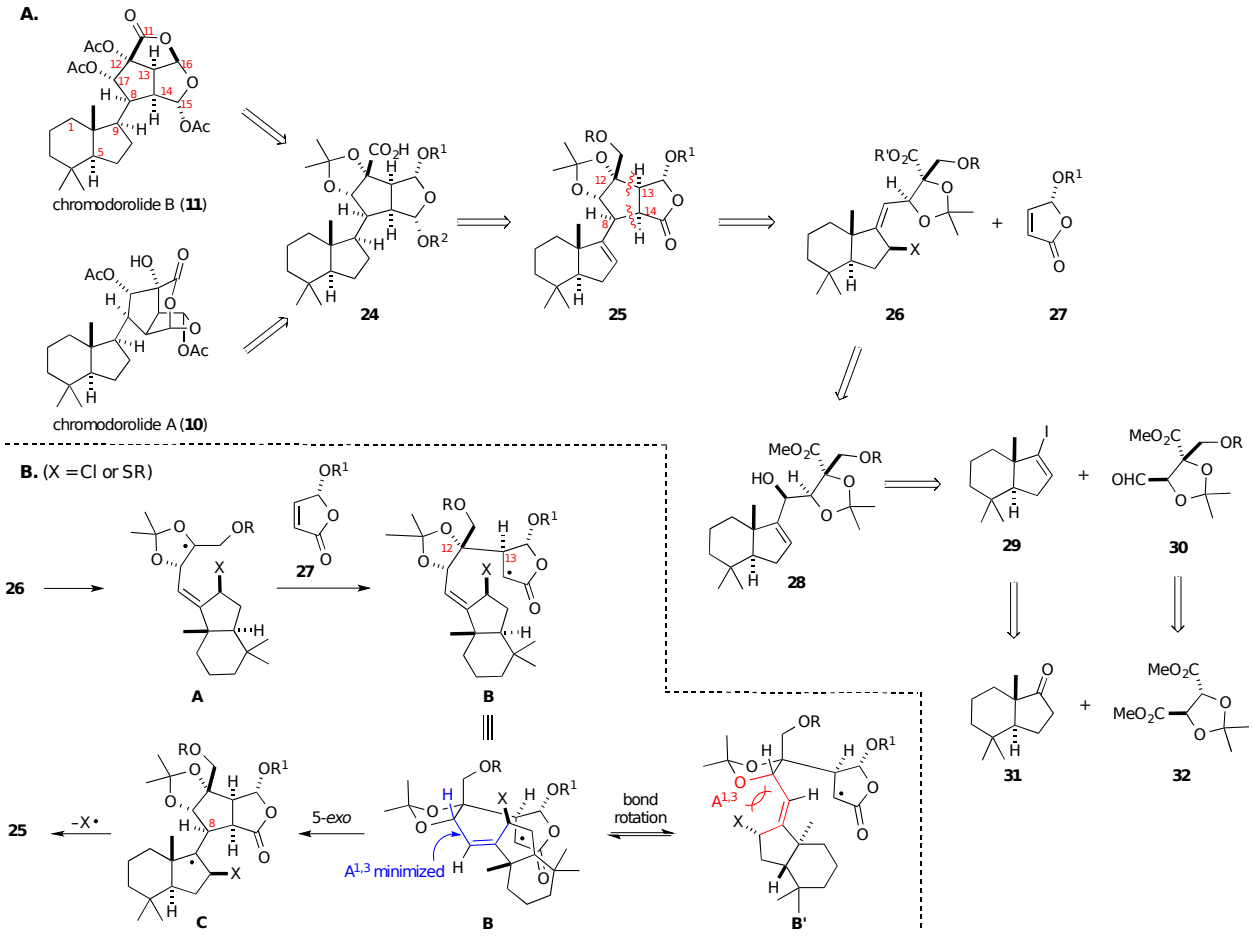


**Figure 2. A.** Plan for the proposed synthesis of chromodorolides B and A. **B.** Mechanistic analysis of the central radical addition/cyclization/fragmentation cascade to form pentacyclic intermediate **25**.

to hydrindene **25**, with the expectation that late-stage hydrogenation of its double bond would take place from the face opposite the angular methyl substituent to install the C-9 stereocenter. We were attracted to a carbon radical-based approach to construct **25**, which we expected to be compatible with pre-installed oxygen functionalities at C-11, C-12 and C-17.[28,29] The cyclopentane ring of key intermediate **25**, we saw arising in one step from the union of tricyclic acetonide carboxylate **26** and (*R*)-5-alkoxybutenolide **27**.[30] We envisioned the *trans*-hydrindane acetonide **26** evolving from allylic alcohol **28**, which in turn would result from the addition of a vinylic nucleophile generated from vinyl iodide **29** and aldehyde **30**. As (*S*,*S*)-trimethylhydrindanone **31**[31] is the obvious precursor of iodide **29**, and (*R*,*R*)-tartaric acid derived acetonide **32** of aldehyde **30**,[32] the plan outlined in Figure 2A projects assembling the chromodorolides from three well known enantiopure starting materials: **27**, **31**, and **32**.

In the projected cascade sequence,[5] chiral acetonide (2,2-dimethyl-1,3-dioxolane) radical **A**, formed from oxidative decarboxylation of precursor **26**, would couple with butenolide **27** to generate alkoxyacyl radical **B** which would undergo 5-*exo* cyclization with the proximal alkene to generate intermediate **C** (Figure 2B). The radical cascade would then be terminated by $\beta$-fragmentation of the C–X bond (X = Cl or SR) of this intermediate to yield pentacyclic product **25**. If successful, the proposed bimolecular radical addition/cyclization/fragmentation (ACF) cascade would form two C–C bonds and four contiguous stereocenters of the chromodorolides in a single step. The stereochemical outcome of two steps would be critical to the efficiency of the proposed cascade sequence (Figure 2B). First, the Giese reaction to unite acetonide radical **A** with butenolide **27** would have to correctly set the C-12 and C-13 stereocenters.[33,34] Ample precedent existed that this union would take place from the butenolide face opposite to the alkoxy group to correctly set the C-13 stereocenter.[35] Less certain would be the facial selectivity of the reaction of trisubstituted acetonide radical **A**. To correctly form the C-12 stereocenter, this coupling would have to take place from the acetonide radical face proximal to the vinylic β-substituent. As few C–C bond-forming reactions of 2,2-dimethyl-1,3-dioxolane trisubstituted radicals had been described, with both *syn*- and *anti*-addition being observed,[36] it was uncertain at the outset from which face radical intermediate **A** would couple. We took some encouragement from the report by Renaud that a bulky β-substituent (*tert*-butyl)

favored bond formation *cis* to the substituent, although in these precedents the alkene was unsubstituted at its bond-forming terminus.[36a] The second step whose stereochemical outcome would be critical is the 5-*exo* cyclization of tetracyclic radical intermediate **B**. We expected that this conversion would take place as depicted in Figure 2B by a conformation that minimizes destabilizing $A^{1,3}$ interactions.

As we had most concern about the facial selectivity in the bimolecular radical coupling step, particularly with regard to facial selectivity of the reaction of a trisubstituted acetonide radical, we chose to examine this aspect of the ACF cascade in a model system having a terminal alkyne substituent at the β carbon of the acetonide radical (Scheme 3). Starting with *L*-arabinose (**33**), enantiopure *N*-acyloxyphthalimide **35** was prepared in 10 steps by way of the known acetonide alcohol **34**.[37,38] Using a slight modification[39] of visible-light photoredox conditions pioneered by Okada for generating radicals from *N*-acyloxyphthalimides,[40] the coupling of **35** with 2.2 equiv of enantiopure (*R*)-5-*L*-menthoxybutenolide (**36**)[30b,c] gave the crystalline tricyclic lactone **37** in 38% yield. X-ray analysis of **37** confirmed that the coupling step had taken place as desired.[26b] The other isolable product, formed in 7% yield, was **38**. $^1$H NMR NOE analysis confirmed that this product formed from coupling of the trisubstituted acetonide radical from the face opposite to the alkyne substituent, resulting in the coupled radical being quenched rather than undergoing 5-*exo* cyclization with the *trans*-oriented alkyne substituent. In subsequent studies published elsewhere, the coupling of a broad selection of trisubstituted acetonide radicals harboring β-substituents was studied both experimentally and computationally.[41] The origin of the observed *syn* stereoselection for the addition of the trisubstituted radical formed from **35** to butenolides such as **36** is ascribed to destabilizing non-covalent interactions between the alkynyl substituent and silyl-protected hydroxymethyl substituent in the transition state.[36a,41] Since the β-substituent of the trisubstituted radical **A** (Figure 2B) in the proposed ACF cascade is certainly larger than an alkyne, we were encouraged to proceed ahead to assemble the fragments to examine this pivotal step in our synthesis plan.

**Scheme 3**

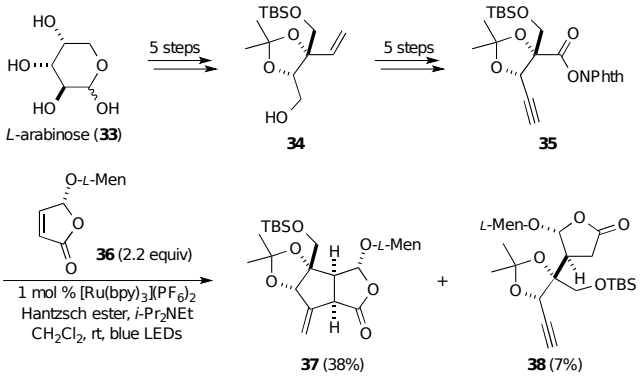


**Synthesis of (*S*,*S*)-Trimethylhydrindanone 31 and Vinyl Iodide 29.** Several syntheses of enantioenriched *trans*-hydrindanone **31** have been reported.[31] We initially examined the short route reported by Granger and Snapper to prepare this ketone from 2-methylcyclopenten-2-one and prenylmagnesium bromide.[31b] After slight modification, this approach provided initial quantities of (*S*,*S*)-*trans*-hydrindanone **31** for our early studies. However, this route was deemed impractical for a large-scale preparation of **31** because of its modest overall yield (20%) and scalability issues in several steps.[37]

We turned to examine a biomimetically inspired polyene cyclization route to *trans*-hydrindanone **31**.[42] Based on the reports from the Yamamoto[43] and Corey[44] laboratories, we conjectured that dienyne **39**, obtained in two steps from geranyl chloride,[37] would undergo enantioselective proton-initiated polyene cyclization upon exposure to a chiral BINOL derivative in the presence of a strong Lewis acid, forming the alkylidene *trans*-hydrindane **42b** (Scheme 4).[45] In our hands, subjection of dienyne **39** to the reaction conditions reported by Corey,[44] using $SbCl_5$ in combination with (*R*)-*o,o'*-dichloro-BINOL **41** (X = Cl) led to a 1:3 mixture of two regioisomeric bicyclic products **42a** and **42b** in 35% combined yield (entry 1). Ozone-mediated cleavage of the exocyclic double bond of **42b** provided racemic *trans*-hydrindanone **31**. Examination of other Lewis acids (entries 2 and 3) revealed $SnCl_4$ to be superior in terms of reaction efficiency and enantioinduction. Unfortunately, further variation of reaction temperatures and the use of unsubstituted BINOL (**41**, X = H) led to no appreciable improvements in enantioselectivity or selectivity in forming **42b** (entries 4–6). Unable to eliminate formation of the *trans*-decalin product **42a**, we examined cyclization of propargylic silane **40**.[46] However, reactions of this precursor gave **43** in low yield only (e.g., entry 7).[47]

**Scheme 4**

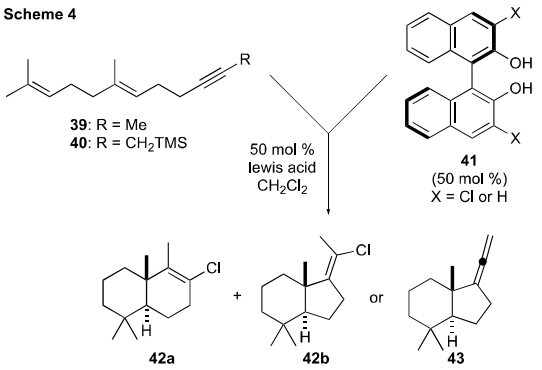


| entry | Lewis acid | R | X | T (ºC) | yield[a] (ratio **42a**:**42b**)[b] | **31**, %ee[c] |
|---|---|---|---|---|---|---|
| 1 | $SbCl_5$ | Me | Cl | –78 | 35% (1.0:3.0) | 0% |
| 2 | $TiCl_4$ | Me | Cl | –78 | <5% (*ND*) | *ND* |
| 3 | $SnCl_4$ | Me | Cl | –78 | 55% (1.0:1.5) | 18% |
| 4 | $SnCl_4$ | Me | Cl | –90 | 53% (1.0:1.1) | 20% |
| 5 | $SnCl_4$ | Me | Cl | –50 | 12% (0:1.0) | *ND* |
| 6 | $SnCl_4$ | Me | H | –78 | 53% (1.1:1.0) | 13% |
| 7 | $SnCl_4$ | $CH_2TMS$ | Cl | –78 | 23% (0:1.0) | *ND* |

[a]Isolated combined yield of **42a** and **42b.** [b]Determined by $^1H$ NMR integration of the crude reaction mixture. [c]Hydrindanone **31** was obtained by ozonolysis of **42b** or **43.** Enantioselective HPLC analysis of a hydrazone derivative was used to establish enantiopurity of **31**.[37]

The scalable route we finally developed to provide (*S*,*S*)-*trans*-hydrindanone **31** is summarized in Scheme 5. This sequence hinged on stereospecific reductive transposition of an allylic alcohol intermediate to set the thermodynamically disfavored *trans* ring fusion of **31**.[48,49] The preparation begins with commercially available (*S*)-enedione **44**,[50] which alternatively can be obtained reliably in 98% *ee* on >20 g scales in two steps from 2-methylcyclopentane-1,3-dione.[51] Selective ketalization of **44**, followed by stereoselective 1,2-reduction of the enone provided allylic alcohol **45** in 98% yield after a simple distillation. A number of approaches were investigated to convert allylic alcohol **45** to the desired *trans*-hydrindene ketal **48**. Treatment of **45** with *o*-nitrobenzenesulfonylhydrazine followed by warming of the reaction to room temperature, as described by Myers,[52] led to the desired *trans*-fused ketal **48** as a minor component of a complex mixture of product. Unable to perform the desired transformation in a single step, we turned to examine Tsuji's palladium-mediated stereospecific reductive transpositions of $\beta$-allylic carbonates and formates.[49] Carbonate **46** readily underwent the desired reductive transposition upon treatment with $Pd(acac)_2$, $(n\text{-}Bu)_3P$, and finely crushed $NH_4HCO_2$ to provide *trans*-hydrindene ketal **48** in 77% yield. The choice of phosphine was critical to the success of the reaction, as the use of other phosphines ($Cy_3P$, $t\text{-}Bu_3P$, $Ph_3P$) led largely to recovery of starting carbonate. The more commonly used allylic formate,[49] **47**, was found to be inert under our reaction conditions. Stereoselective cyclopropanation of the trisubstituted double bond of **48** was achieved by reaction with diethylzinc and chloroiodomethane,[53] which after acidic workup delivered cyclopropyl ketone **49** in 92% yield. It was important to use chloroiodomethane in this reaction, as use of diiodomethane led largely to recovery of the starting alkene. Hydrogenolysis of cyclopropane **49** using $PtO_2$ in acetic acid,[54] followed by PCC oxidation of the resulting secondary alcohol gave *trans*-hydrindanone **31** in 88% yield over two steps. This sequence delivered (*S*,*S*)-*trans*-hydrindanone **31** (98% ee) in 7 steps and 59% overall yield from enone **44**. Using the method of Barton,[55] hydrindanone **31** was converted to the known vinyl iodide **29**[31a] in 78% yield. The sequence summarized in Scheme 5 readily provided 7 g of the light-sensitive iodide **29** in a single pass.

**Scheme 5**

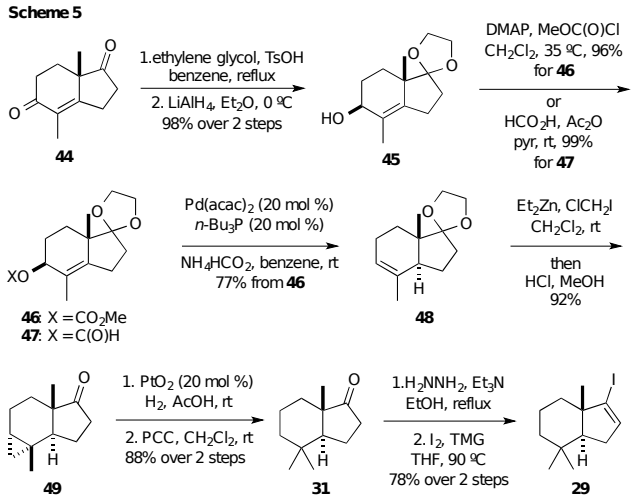


**Synthesis of Aldehyde 30 and its Coupling with a *trans*-Hydrindene Nucleophile.** With streamlined access to vinyl iodide **29** in hand, we turned our attention to the synthesis of the aldehyde coupling partner **30** (Scheme 6). The sequence began with tartrate-derived acetonide **32**, which was desymmetrized by LDA-mediated alkylation with BOM-Cl, as reported by Crich, to give benzyl ether **50** in 46% yield.[32,56,57] Selective reduction of the less hindered ester group of **50** with DIBALH provided primary alcohol **51** in 45% yield along with 36% of recovered starting material **50**. All our attempts to improve the efficiency of this conversion were unsuccessful, as the use of alternate reductants (e.g., $LiAlH_4$, Red-Al) or extra equivalents of DIBALH led to complex mixtures of various reduction products. Oxidation of primary alcohol **51** to aldehyde **30** could be achieved by a number of conventional methods; however, purification of **30** proved to be challenging. We ultimately elected to oxidize alcohol **51** with the Dess-Martin reagent (DMP) in $CH_2Cl_2$ and filter the resulting mixture with *n*-hexanes over Celite to remove the insoluble byproducts and give aldehyde **30** in 93% yield and high purity.[58] As a result of its unexpected instability, aldehyde **30** was used immediately in the ensuing coupling step (*vide infra*).[59] This proved to be a short and

scalable approach to aldehyde coupling partner **30**, with >8 g being readily prepared in a single pass, albeit in modest overall yield.

**Scheme 6**

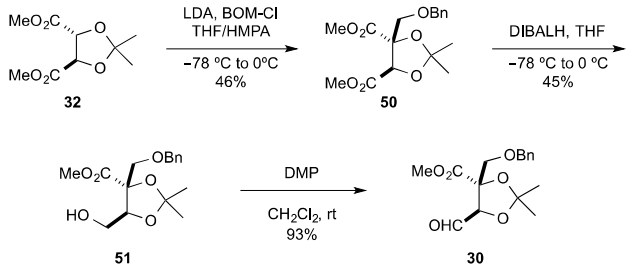


Next, we focused on uniting the *trans*-hydrindene and aldehyde fragments. Early attempts to directly couple the vinyllithium intermediate formed from vinyl iodide **29** with aldehyde **30** provided low yields (<20% yields) of adducts as an equimolar mixture of allylic alcohol epimers. We turned to the use of the Nozaki-Hiyama-Kishi (NHK reaction) to achieve the desired fragment-coupling (Scheme 7).[60] Conditions that had been employed earlier to couple this iodide[61] led to the formation of adduct **52** in low yields and 3:1 stereoselectivity. To accelerate the rate of NHK coupling and improve stereoselection, we elected to employ the oxazoline ligands developed by the Kishi group.[62] To our delight, use of ligand (*R*)-**53** resulted in the formation of adduct **52** as a single diastereomer in 28% yield. The identical reaction using the enantiomeric ligand, led to inversion of diastereoselectivity, giving the allylic alcohol epimer in 18% yield and 4:1 dr. Upon further optimization of the reaction with ligand (*R*)-**53**, we discovered that employing the sensitive aldehyde **30** in a slight excess (1.6 equiv) and performing the reaction on a larger scale (3 mmol) led to the formation of the desired product **52** in 66% isolated yield.[63]

**Scheme 7**

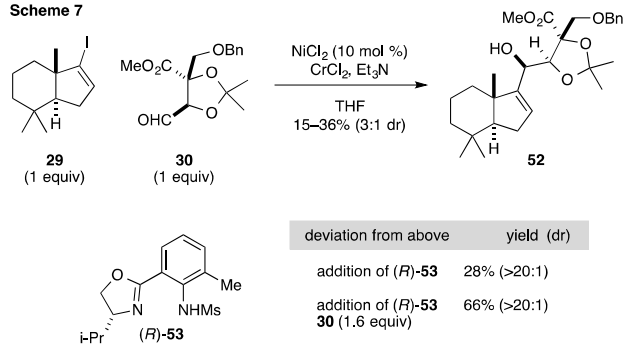


| deviation from above | yield (dr) |
|---|---|
| addition of (*R*)-**53** | 28% (>20:1) |
| addition of (*R*)-**53** **30** (1.6 equiv) | 66% (>20:1) |

Having forged all of the C-C bonds of the radical cascade precursor, efforts were focused on allylic transposition of the alcohol functionality to a heteroatom capable of undergoing radical β-cleavage, while setting the required *E*-configuration of the exocyclic double bond of the product (Scheme 8). We first investigated the possibility of performing a [3,3]-sigmatropic rearrangement to an allylic thiocarbonate.[64,65] To this end, deprotonation of alcohol **52** with KHMDS at -78 ºC, followed by addition of phenyl chlorothionoformate (**54**) resulted in thioacylation and spontaneous [3,3]-sigmatropic rearrangement upon warming to room temperature to give allylic thiocarbonate **55** as a single stereoisomer in 68% yield. However, we were unable to selectively cleave the methyl ester group of **55** in the presence of the sensitive thiocarbonate functionality under a variety of classical saponification, $S_N2$ demethylation,[66] or other non-basic methods.[67] To circumvent this selectivity issue, the order of transformations was reversed. Saponification of methyl ester **52** and subsequent esterification with *N*-hydroxyphthalimide (NHP) provided the crystalline NHP ester **56** in 69% yield, whose structure was confirmed by single-crystal X-ray analysis.[26c] Unfortunately, subjection of allylic alcohol **56** to the reaction conditions that were successful for thioacylation of **52** led to immediate decomposition of the *N*-acyloxyphthalimide functionality.[68] Deprotonation of **56** with LiHMDS or NaHMDS followed by reaction with **54** led to recovery of the starting material, whereas reaction of **56** with other potassium bases uniformly resulted in instantaneous decomposition. Unable to selectively activate hindered allylic alcohol **56** for thioacylation with phenyl chlorothionoformate (**54**), we turned to investigating allylic OH → Cl transformations. Reaction of alcohol **56** with 2 equiv of $SOCl_2$ in a 10:1 mixture of $Et_2O$/pyridine at –40 ºC induced the desired suprafacial rearrangement to deliver crystalline *N*-acyloxyphthalimide radical precursor **57**,[69] whose structure was confirmed by single-crystal X-ray analysis,[26d] in 62% yield on gram-scale. This stereoselective conversion could also be accomplished on the product of the NHK coupling **52**, followed by saponification to the corresponding carboxylic acid. However, in contrast to NHP ester **57**, the non-crystalline acid produced was difficult to purify.

**Scheme 8**

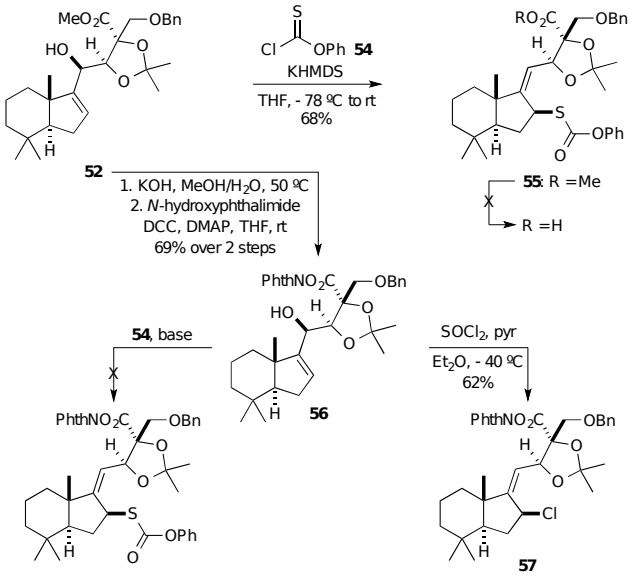


**Initial Exploration of the ACF Radical Cascade.** Exposure of *N*-acyloxyphthalimide **57** to standard reductive photoredox reaction conditions[39] in the presence of 4 equiv of enantioenriched (89% *ee*) (*R*)-5-methoxybutenolide (**58**)[30a,c] gave a mixture of four products accounting for 95% of the mass balance (Scheme 9, entry 1). Pentacyclic products **62** (35%) and **63** (25%) arose from the desired ACF cascade reaction. Initial structural assignments of products **62** and **63** were based on detailed analyses of their NMR spectra. Particularly useful were $^1$H NOE correlations between the C-8, C-17, and C-14 methine hydrogens.[37] Further confirmation of the structures of these two C-8 epimers was obtained by eventual conversion of cascade product **63** to (-)-chromodorolide B (**11**). The stereochemical relationship of lactone and hydrophobic fragments in the two tetracyclic products was assigned based on a strong $^1$H NOE correlation between the C-17 methine hydrogen and the C-11 hydrogens of the benzyloxymethyl substituent of isomer **61**. Products **61**, **62** and **63** are derived from the desired *syn* addition of butenolide **58** to the acetonide radical formed from **57**. In contrast, tetracyclic lactone **60** arose from coupling of the dioxolane radical with acceptor **57** *anti* to the vicinal hydrophobic fragment. The resulting *R* configuration at C-12 prevents ensuing 5-*exo* cyclization.[70]

Although the initial coupling of dioxolane radical to butenolide **58** occurred with 7.6:1 diastereoselectivity favoring the desired adduct, minimizing premature reduction of the $\alpha$-acyl radical intermediate leading to the significant byproduct, lactone **61**, would be important for optimizing the efficiency of the ACF cascade. Formation of product **61** indicated that quenching of the $\alpha$-acyl radical produced in the Giese coupling step by either single-electron transfer (SET) to form an enolate followed by protonation or by hydrogen atom abstraction from Hantzsch ester **59** was competitive with 5-*exo* cyclization.[39] In an attempt to minimize the SET pathway,[39] *i*-$Pr_2NEt$ was omitted from the reaction mixture, significantly decreasing the yield of product **61** to 14% (entry 2). To further reduce premature quenching of the radical intermediate, we performed the reaction at higher dilution, resulting in a further decrease in the yield of product **61** to 3% (entry 3). However, these more dilute conditions also resulted in less efficient coupling of the dioxolane radical and butenolide **58** leading to lower yields of pentacyclic products **62** and **63**. To attenuate hydrogen atom abstraction by the $\alpha$-acyl radical in reactions carried out at higher concentration, we employed 4,4-dideuterio analogue of Hantzsch ester **59** (entry 4). Under these conditions, the combined yield of cyclization products **62** and **63** increased to 70%, with tetracyclic lactone **61** being formed in only 6% yield.

Having attenuated premature quenching of the $\alpha$-acyl radical intermediate, we sought to explore the effects of temperature, solvent, and structural modifications of butenolide **58** on diastereoselection of the 5-*exo* cyclization. As illustrated in Scheme 9, the major pentacyclic product **62** arose from cyclization taking place by a transition state related to radical conformer **D**, not by way of a transition structure related to conformer **E**. Varying the temperature of the reaction (0 ºC to 40 ºC) did not have a significant impact on the ratio of the epimeric products **62** and **63**. Likewise, using butenolides harboring acetoxy or menthoxy substituents at the acetal stereocenter, led to no improvement in the yield of the desired tetracyclic product **63**. The ratio was slightly enhanced in reactions conducted in acetonitrile, allowing the desired epimer **63** to be isolated in 27% yield (entry 5). Unable to further increase the yield of the desired ACF product **63**, we decided to advance pentacycle forward to validate our post fragment-coupling strategy.

**Scheme 9**

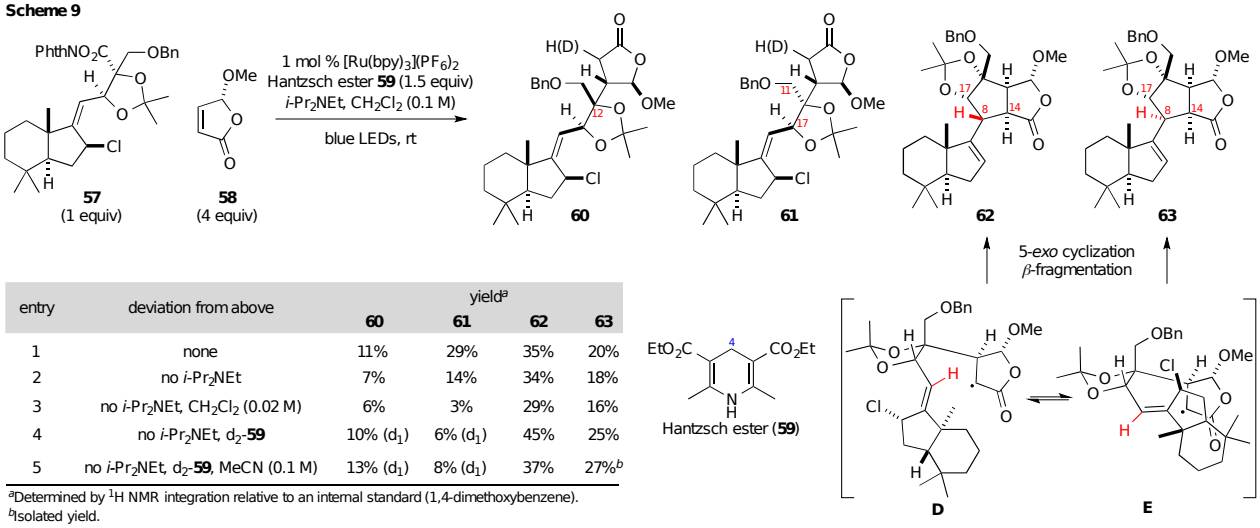


| entry | deviation from above | yield[a] 60 | 61 | 62 | 63 |
|---|---|---|---|---|---|
| 1 | none | 11% | 29% | 35% | 20% |
| 2 | no *i*-$Pr_2NEt$ | 7% | 14% | 34% | 18% |
| 3 | no *i*-$Pr_2NEt$, $CH_2Cl_2$ (0.02 M) | 6% | 3% | 29% | 16% |
| 4 | no *i*-$Pr_2NEt$, $d_2$-**59** | 10% ($d_1$) | 6% ($d_1$) | 45% | 25% |
| 5 | no *i*-$Pr_2NEt$, $d_2$-**59**, MeCN (0.1 M) | 13% ($d_1$) | 8% ($d_1$) | 37% | 27%[b] |

[a]Determined by $^1H$ NMR integration relative to an internal standard (1,4-dimethoxybenzene). [b]Isolated yield.

**Completion of a First-Generation Total Synthesis of (-)-chromodorolide B**. Product **63** of the ACF cascade was converted to (–)-chromodorolide B (**11**) by way of two isolated and purified intermediates, **64** and **65** (Scheme 10). Reduction of **63** with DIBALH at –78 ºC and *in situ* acetylation with $Ac_2O$ and DMAP afforded diacetal **64** as a single epimer at C-15,[71] which was assigned the $\alpha$-orientation on the basis of $^1H$ NOE correlations between the C-15 and C-17 methines. We speculate that stereoselection in this reduction resulted from prior coordination of DIBALH with the benzyl ether substituent. Following unsuccessful attempts to accomplish reduction of the alkene and deprotection of the benzyl ether in one step, we first unveiled the primary alcohol under transfer-hydrogenation conditions, followed by conventional $PtO_2$-mediated alkene hydrogenation. The latter step proceeded exclusively from the alkene face opposite the angular methyl group to afford a single product **65** in 86% yield. Without purifying subsequent intermediates, the primary alcohol of **65** was oxidized to carboxylic acid **66**, which upon exposure of the crude reaction mixture to 1:1 solution of 4 M HCl and THF for 72 h at room temperature delivered pentacyclic intermediate **67** as a mixture of lactol epimers. Reaction of a pyridine solution of this intermediate with a large excess of acetic anhydride in the presence of DMAP gave (-)-chromodorolide B (**11**) as a colorless solid in 49% overall yield from tetracyclic alcohol precursor **65**. Spectroscopic data for synthetic **11** compared well with that reported for the natural product.[17b] The magnitude of the levorotatory rotation, $[\alpha]_D$ = -67 ($c$ = 0.12, $CH_2Cl_2$), was somewhat less than that reported, $[\alpha]_D$ = -95 ($c$ = 0.12, $CH_2Cl_2$), for a non-crystalline sample of the natural product.[17b] Recrystallization of synthetic (-)-chromodorolide B (**11**) provided single crystals, mp = 236–238 °C, allowing its structure to be unambiguously confirmed by X-ray analysis.[26e]

**Scheme 10**

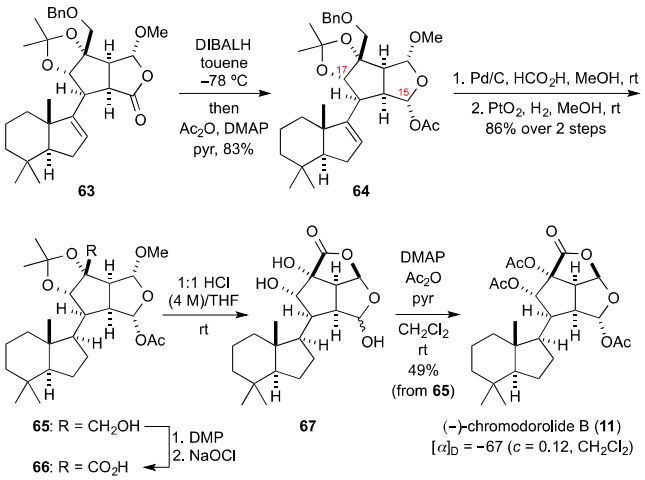


**Computational Analysis of Stereoselection in the 5-exo Radical Cyclization Step of ACF Cascade.** As discussed earlier, we had predicted erroneously that the 5-*exo* cyclization in the ACF cascade would occur preferentially from a conformation wherein $A^{1,3}$ interactions would dictate which face of the alkene would be attacked. In an attempt to gain insight into the observed stereoselection of this step, we analyzed the origin of the stereoselectivity computationally. Two mechanistic scenarios for the 5-*exo* cyclization were considered: (1) direct cyclization of an $\alpha$-acyl radical onto the pendant alkene (the scenario outlined in Figure 2 and Scheme 9), and (2) initial SET to the radical intermediate formed in the bimolecular coupling step to form a lactone enolate that subsequently undergoes $S_N2'$ cyclization. To identify the most likely pathway, energies and structures of diastereomeric transition states for the stereochemistry determining step of both modes of cyclization were computed using the TPSS[72a] and TPSSh[72b] functionals and the def2-TZVP basis sets[73] in combination with the BJ-damped D3-disperion correction.[74,75] In the case of the radical pathway, the lowest-energy transition state, **TS-**

**A-*trans***, leading to the undesired C-8 epimer **62**, was found to be 1.0 kcal/mol (in $CH_2Cl_2$) or 0.5 kcal/mol (in MeCN) lower in energy than **TS-A-*cis*** leading to epimer **63** having the C-8 configuration of (–)-chromodorolide B. The computed ratio of cyclized products **62**:**63** of 2.5:1 in MeCN agreed reasonably well with the experimentally observed ratio of 1.4:1. In contrast, computed diastereomeric transition states for the polar reaction pathway (enolate formation followed by concerted $S_N2'$ cyclization, Supporting Information Figure S2) found the transition state leading to product **63** to be lower in energy by 0.7 kcal/mol (in MeCN) or 0.5 kcal/mol (in $CH_2Cl_2$). Although the energy differences of the computed diastereoisomeric transitions states in the two mechanisms are small, the radical pathway, which we consider the most plausible, was more consistent with the observed reaction outcome. As a result, further computational studies focused on this pathway.

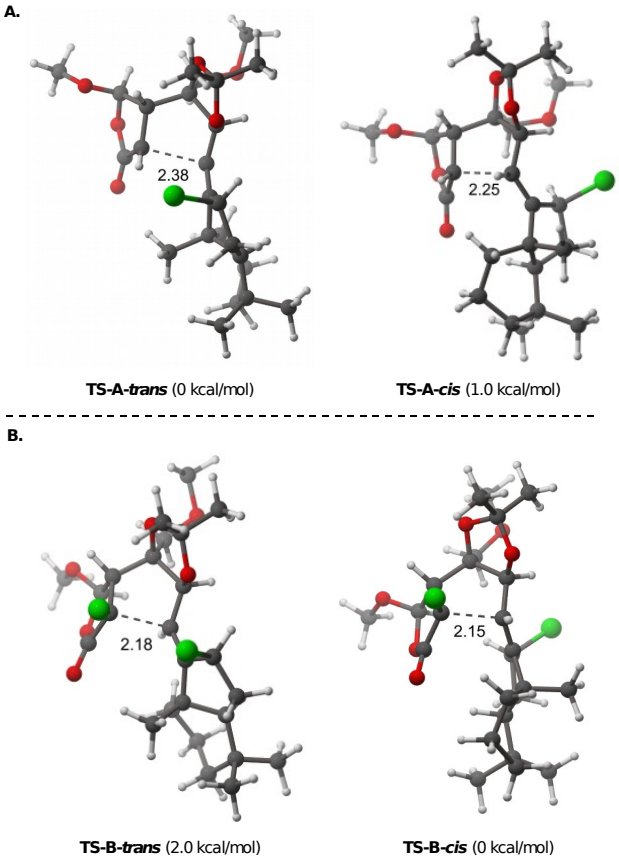


**Figure 3**. Structures and energies of diastereoisomeric transition states of the 5-*exo* radical cyclization step of the ACF cascade. **A.** For the intermediate generated by addition of the acetonide radical to (*R*)-5-methoxybutenolide. **B.** For the intermediate generated by addition of the acetonide radical to (*R*)-3-chloro-5-methoxybutenolide. Values enclosed in parentheses are relative energies computed using the TPSS functional and def2-TZVP basis set ($CH_2Cl_2$ solvent); the values by the dotted line are the lengths of the forming C–C bond in Å. The transition structures labeled "*cis*" lead to the formation of the configuration at C-8 found in (–)-chromodorolide B. To reduce computation time, the benzyloxy substituent at C-11 was replaced with methoxy.

Examination of the transition structures of the two diastereomeric transition states of the radical pathway (Figure 3A) was instructive. The lower-energy diastereomeric transition structure, **TS-A-*trans***, has a longer forming bond (2.38 vs 2.25 Å) and a somewhat helical shape. Further analysis suggested a potential destabilizing steric interaction between the chloride of the hydrindane fragment and a substituent larger than hydrogen at the $\alpha$-carbon of the butenolide fragment in a transition structure analogous to **TS-A-*trans***. If the $\alpha$-carbon of the butenolide carried a chloride or bromide substituent, the halogen substituents would clash a helical *trans*-transition structure, yet would point in opposite directions in a *cis*-transition structure. In addition, introduction of a halogen should shift the transition states later by decreasing the nucleophilicity of the butenolide radical, which could further increase a destabilizing halogen-halogen interaction.

The computationally predicted lowest energy transition structures for the 3-chloride analogue are shown in Figure 3B. As envisioned, the **TS-B-*trans*** is affected significantly, with the forming C–C bond distance decreased from 2.38 Å to 2.18 Å. As a consequence, the kinetic barrier for forming the *trans* product is increased from 7.9 kcal/mol to 11.3 kcal/mol (Supporting Information Figure S5). The forming bond in **TS-B *cis*** is also shortened slightly (from 2.25 Å to 2.15 Å) and the kinetic barrier slightly is increased from 8.9 kcal/mol to 9.4 kcal/mol. The transition state that would lead to the ACF product having the C-8 configuration of (–)-chromodorolide B, **TS-B-*cis***, is now predicted to be more stable by 1.9 kcal/mol. For the bromide analogue, the selectivity is predicted to be even slightly higher (Table 1).[76]

**Table 1. The relative Gibbs free energies of TS-*cis* and TS-*trans* for α-H, α-Cl and α-Br butenolide substrates in $CH_2Cl_2$.**

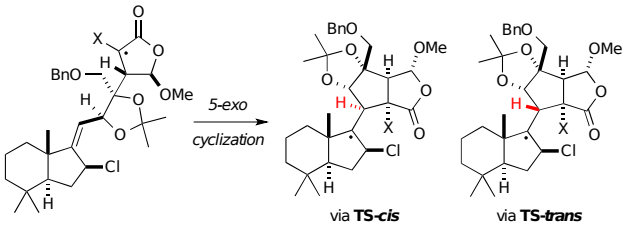


| functional | ΔG(TS-*cis*–TS-*trans*), kcal/mol | | |
|---|---|---|---|
| | X = H | X = Cl | X = Br |
| TPSS-D3 | 1.0 | –1.9 | –2.4 |

**Second-Generation Total Synthesis of (–)-Chromodorolide B by Way of a Stereoselective ACF Cascade.** We opted to explore this computational prediction by utilizing a 3-chlorobutenolide in the radical coupling step.[77] This possibility was particularly attractive, as we have shown previously that the addition of a 3-Cl substituent to a butenolide increases the yields of radical coupling reactions, and in addition the α-chloride substituent in a coupled product can be removed directly in the photoredox-catalyzed coupling step.[2b] Salient results of our investigation of the use of enantiopure 3-chlorobutenolide **68**[2b] in the ACF cascade are summarized in Table 2. Using the reaction conditions optimized earlier (entry 5, Scheme 9) and carrying out the reaction with 1 equiv of both *N*-acyloxyphthalimide **57** and chlorobutenolide **68**, followed by addition of *n*-$Bu_3N$ and additional irradiation to promote dechlorination,[2b,78] provided an ACF cascade product that still contained the chloride substituent. Hypothesizing that under these conditions the dechlorination step was slow, the crude product after aqueous extraction was isolated and re-subjected to dechlorination using *n*-$Bu_3N$ and the iridium photocatalyst, $Ir[dF(CF_3)ppy]_2(dtbbpy)PF_6$. This sequence provided a single ACF cascade product **69** in 41% yield (Table 2, entry 1). The pentacyclic C-8 epimer of **69** was not detectable by NMR analysis. Increasing the concentration of the reaction to 0.6 M led to ACF product **69** being formed in 58% yield (entry 2). We eventually found that the desired cascade sequence and dechlorination of the product could be accomplished in a single step by utilizing 2 mol % of $Ir[dF(CF_3)ppy]_2(dtbbpy)PF_6$ as the sole photocatalyst (entry 3). The yield of **69** was similar using Hantzsch ester **59** (entry 4), which was expected as by-products resulting from premature quenching of the α-acyloxy radical intermediate had not been observed. In addition, we were able to use an organic photocatalyst, 4CzIPN,[79-81] in place of the Ir catalyst, giving the desired ACF cascade product in 54% isolated yield (entry 5). Thus, the computationally-guided structural modification of the butenolide coupling partner resulted in doubling the yield of the pivotal pentacyclic intermediate **69** and decreasing the amount of butenolide acceptor required in this step by four-fold.

**Table 2. Optimization of the fragment coupling between NHP ester 57 and chlorobutenolide 68.**

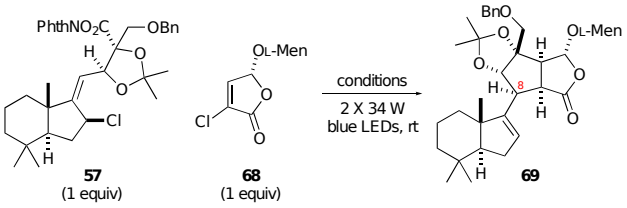


**57** (1 equiv) **68** (1 equiv) **69**

| entry | conditions | isolated yield |
|---|---|---|
| 1 | (a) 2 mol % $[Ru(bpy)_3](PF_6)_2$, $d_2$-Hantzsch ester **59**, MeCN (0.1 M) (b) 2 mol % $Ir[dF(CF_3)ppy]_2(dtbbpy)PF_6$, *n*-$Bu_3N$, THF (0.1 M) | 41% |
| 2 | (a) 2 mol % $[Ru(bpy)_3](PF_6)_2$, $d_2$-Hantzsch ester **59**, MeCN (0.6 M) (b) 2 mol % $Ir[dF(CF_3)ppy]_2(dtbbpy)PF_6$, *n*-$Bu_3N$, THF (0.1 M) | 58% |
| 3 | 2 mol % $Ir[dF(CF_3)ppy]_2(dtbbpy)PF_6$, $d_2$-Hantzsch ester **59**, THF (0.6 M), then $Bu_3N$ | 56% |
| 4 | 2 mol % $Ir[dF(CF_3)ppy]_2(dtbbpy)PF_6$, Hantzsch ester **59**, THF (0.6 M), then $Bu_3N$ | 57% |
| 5 | 2 mol % 4CzIPN, Hantzsch ester **59**, THF (0.6 M), then $Bu_3N$ | 54% |

To confirm that the chlorine, and not the menthoxy, substituent was responsible for the high stereoselection observed in the fragment coupling summarized in Table 2, we examined the reaction of NHP ester **57** with 3-chloro-5-methoxybutenolide. Although this butenolide is not available in enantioenriched form,[2b] this investigation could be carried out using racemic 3-chloro-5-methoxybutenolide (**70**),[82] as authentic samples of the diastereomeric ACF products **62** and **63** were available. As summarized in eq 1, the reaction of NHP ester **57** with racemic butenolide **70** provided **63** as the major product, with no trace of its C-8 epimer, **62**, being seen by careful $^1H$ NMR analysis of the crude reaction mixture[37]

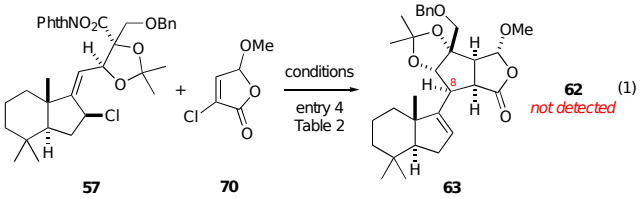


**57** (1 equiv) **70** *racemic* (1 equiv) **63** *major product* **62** (1)

With sufficient amounts of lactone **69** in hand, we elaborated it to (-)-chromodorolide B (**11**) by a seven-step sequence that paralleled the final steps of our first-generation synthesis (Scheme 11). Reduction of lactone functionality of **69** and *in situ* acetylation of the resulting aluminum hemiacetal intermediate with $Ac_2O$ proceeded smoothly to deliver diacetal **71** in 98% yield.

Deprotection of the primary alcohol proved challenging once again. Debenzylation of **71** employing the acidic transfer hydrogenolysis conditions developed during our first-generation synthesis of **11**, resulted in cyclization of the newly unveiled C-11 alcohol onto C-16 forming a bridging tetrahydrofuran ring. We were able to suppress this undesired cyclization by performing the reaction with basic $Pd(OH)_2$ and $H_2$.[83] Without purification, the trisubstituted alkene was reduced stereoselectively with $PtO_2$ to deliver saturated-pentacyclic product **72** in 88% over two steps. Finally, we successfully converted **72** to (-)-chromodorolide B (**11**) in 45% yield over four steps by the sequence of transformations employed in our first-generation synthesis.

**Scheme 11**

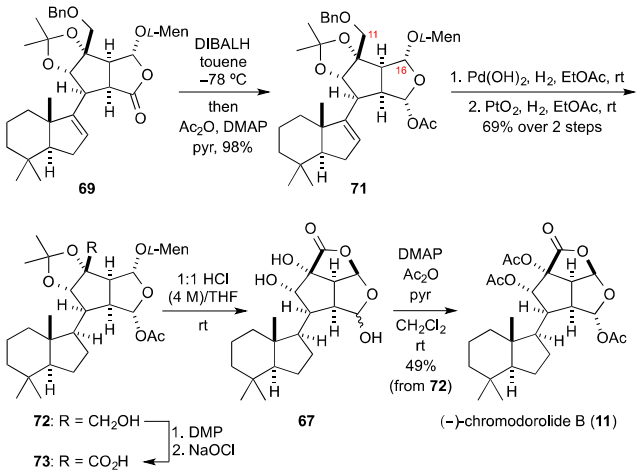


## CONCLUSION

The structurally intricate marine diterpenoid chromodorolide B, which harbors 10 contiguous stereocenters and two chiral attached ring fragments, has been successfully synthesized. This total synthesis establishes the absolute configuration of chromodorolide B, which had previously been proposed on biogenetic grounds. The synthetic sequence features a novel late-stage radical addition/cyclization/fragmentation (ACF) cascade that unites two chiral fragments by forming two C-C bonds and four contiguous stereocenters in a single, highly stereoselective step. A notable feature of this late-stage fragment union is the use of the two coupling partners in equimolar amounts. The coupling step is initiated by visible-light photocatalytic fragmentation of a redox-active ester, which can be accomplished in the presence of 2 mol % of an iridium photocatalyst or 2 mol % of a less-precious electron-rich dicyanobenzene photocatalyst. The high degree of stereocontrol eventually realized in the cascade sequence was made possible by in-depth DFT computational modeling of the 5-*exo* cyclization step of the ACF cascade. Our second-generation total synthesis of (-)-chromodorolide B (**11**) proceeds in in 21 steps from commercially available (*S*)-enedione **44** in 2% overall yield. We anticipate that the results delineated in this study will find applications in future syntheses of other structurally intricate natural products.

## ASSOCIATED CONTENT

### Supporting Information

Experimental procedures, characterization data, and CIF files for X-ray structures of compounds **11**, **23**, **37**, **56**, and **57**. This material is available free of charge via the Internet at http://pubs.acs.org.

### Corresponding Authors

*leoverma@uci.edu

### ORCID

Yuriy Slutskyy: 0000-0002-3059-5362

Mikko Muuronen : 0000-0001-9647-7070

Philipp Kohler: 0000-0002-2424-9527

Larry E. Overman: 0000-0001-9462-0195

### Present Addresses

**D.J.T.**: Process Research and Development, AbbVie Inc., 1 North Waukegan Road, North Chicago, IL 60064.
**M.M.**: BASF SE, Carl-Bosch-Strasse 38, 67056 Ludwigshafen, Germany.
**P.K.**: Process Chemistry R&D, Idorsia Pharmaceuticals Ltd., Hegenheimermattweg 91, CH-4123 Allschwil, Switzerland.

### Notes

The authors declare no competing financial interest.

### ACKNOWLEDGMENTS

Financial support was provided by the U. S. National Science Foundation (CHE1265964 and CHE-1661612) and U. S. National Institute of General Medical Sciences by research grant R01GM098601 and a graduate fellowship award to YS (1F31GM113494). NMR spectra, mass spectra, and X-ray analyses were obtained at UC Irvine using instrumentation acquired with the assistance of NSF and NIH Shared Instrumentation grants. We thank Professor Filipp Furche for hosting M.M. in his laboratory and for his support of the computational studies by the National Science Foundation under CHE-1464828.

### REFERENCES

(1) Ireland, R. E. *Organic Synthesis*; Prentice-Hall: Englewood Hills, N.J., 1969, pp 28–30.
(2) (a) For a brief review of studies in our laboratories, see Jamison, C. R.; Overman, L. E. *Acc. Chem. Res.* **2016**, *49*, 1578–1586. (b) For a recent example, see: Slutskyy, Y.; Jamison, C. R.; Zhao, P.; Lee, J.; Rhee, Y. H.; Overman, L. E. *J. Am. Chem. Soc.* **2017**, *139*, 7192–7195.

(3) For other examples, see: (a) Furst, L.; Narayanam, J. M. R.; Stephenson, C. R. *Angew. Chem., Int. Ed.* **2011**, *50*, 9655–9659. (b) Sun, Y.; Li, R.; Zhang, W.; Li, A. *Angew. Chem., Int. Ed.* **2013**, *52*, 9201–9204.
(4) For selected reviews, see: (a) Tietze, L. F. *Chem. Rev.* **1996**, *96*, 115–136. (b) Tietze, L. F., Brasche, G.; Gericke, K. M. *Domino Reactions in Organic Synthesis*, Wiley-VCH, Weinheim, 2006. (c) Nicolaou, K. C.; Chen, J. S. *Chem. Soc. Rev.* **2009**, *38*, 2993–3009. (d) Pellissier, H. *Chem. Rev.* **2013**, *113*, 442–524. (e) Vavsari, V. F.; Saeed, B. *Curr. Org. Chem.* **2017**, *21*, 1393–1426.
(5) (a) Baralle, A.; Baroudi, A.; Daniel, M.; Fensterbank, L.; Goddard, J.-P., Lacote, E.; Larraufie, M.-H.; Maestri, G.; Malacria, M.; Ollivier, C. In *Encyclopedia of Radicals in Chemistry, Biology and Materials*, Online @ John Wiley & Sons, Ltd., 2012. DOI: 10.1002/9780470971253.rad022. (b) Plesniak, M. P.; Huang, H.-M.; Procter, D. J. *Nat. Rev. Chem.* **2017**, *1*, 77.
(6) For a pioneering example of the alternate sequence–radical cyclization followed by a bimolecular radical coupling, see: Stork, G.; Sher, P.; Chen, H. *J. Am. Chem. Soc.* **1986**, *108*, 6384–6385.
(7) For a preliminary report of a portion of these studies, see: Tao, D. J.; Slutskyy, Y.; Overman, L. E. *J. Am. Chem. Soc.* **2016**, *138*, 2186–2189.

(8) For reviews of rearranged spongian diterpenoids, see: (a) Keyzers, R. A.; Northcote, P. T.; Davies-Coleman, M. T. *Nat. Prod. Rep.* **2006**, *23*, 321–334. (b) González, M. *Cur. Bioact. Compd.* **2007**, *1*, 1–36.

(9) Mayer, A.; Köpke, B.; Anke, H.; Sterner, O. *Phytochem.* **1996**, *43*, 375–376.

(10) Hochlowski, J. E.; Faulkner, D. J.; Matsumoto, G. K.; Clardy, J. *J. Org. Chem.* **1983**, *48*, 1141–1142.
(11) (a) Buckleton, J. S.; Cambie, R. C.; Clark, G. R. *Acta Cryst.* **1991**, *C47*, 1438–1440. (b) Bergquist, P. R.; Bowden, B. F.; Cambie, R. C.; Craw, P. A.; Karuso, P.; Poiner, A.; Taylor, W. C. *Aust. J. Chem.* **1993**, *46*, 623–632. (c) Cheloviolene A was isolated also by Faulkner and Bobzin and called chelonaplysin B, see: Bobzin, S. C.; Faulkner, D. J. *J. Nat. Prod.* **1991**, *54*, 225–232.

(12) Molinski, T. F.; Faulkner, D. J.; Cun-heng, H.; Van Duyne, G. D.; Clardy, J. *J. Org. Chem.* **1986**, *51*, 4564–4567.
(13) Hambley, T. W.; Poiner, A.; Taylor. W. C. *Tetrahedron Lett.* **1986**, *27*, 3281–3282.
(14) Dilip de Silva, E.; Morris, S. A.; Miao, S.; Dumdei, E.; Andersen, R. J. *J. Nat. Prod.* **1991**, *54*, 993–997.
(15) White, A. M.; Pierens, G. K.; Forster, L. C.; Winters, A. E.; Cheney, K. L.; Garson, M. J. *J. Nat. Prod.* **2016**, *79*, 477–483.
(16) Rudi, A.; Kashman, Y. *Tetrahedron* **1990**, *46*, 4019–4022.
(17) Chromodorolide A and B: (a) Dumdei, E. J.; De Silva, E. D.; Andersen, R. J.; Choudhary, M. L.; Clardy, J. *J. Am. Chem. Soc.* **1989**, *111*, 2712–2713. (b) Morris, S. A.; Dilip de Silva, E.; Andersen, R. J. *Can. J. Chem.* **1991**, *69*, 768–771.
(18) Chromodorolide C: Rungprom, W.; Chavasiri, W.; Kokpol, U.; Kotze, A.; Garson, M. J. *Mar. Drugs* **2004**, *2*, 101–107.
(19) Chromodorolide D and E: (a) Uddin, M. H.; Hossain, M. K.; Nigar, M.; Roy, M. C.; Tanaka, J. *Chem. Nat. Compd.* **2012**, *48*, 412–415. (b) Katavic, P. L.; Jumaryatno, P.; Hopper, J. N. A.; Blanchfield, J. T.; Garson, M. J. *Aust. J. Chem.* **2012**, *65*, 531–538.

(20) All natural products having the spongian skeleton are reported to have the absolute configuration depicted in **a**.

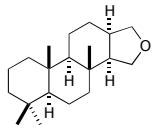

spongian skeleton (**a**)

(21) For leading references to the distinctly different Golgi modifying activities of norrisolide and macfarlandin E, see (a) Takizawa P. A.; Yucel, J. K.; Veit, B.; Faulkner, D. J.; Deerinck, T.; Soto, G.; Ellisman, M.; Malhotra, V. *Cell* **1993**, *73*, 1079–1090. (b) Guizzunti, G.; Brady, T. P.; Fischer, D.; Malhotra, V.; Theodorakis, E. A. *Bioorg. Med. Chem.* **2010**, *18*, 2115–2122. (c) Schnermann, M. J.; Beaudry, C. M.; Egovora, A. V.; Polishchuk, R. S.; Sütterlin, C.; Overman, L. E. *Proc. Nat. Acad. Sci. USA* **2010**, *107,* 6158–6163.
(22) For a study of the reactivity and biological activity of simplified analogues of macfarlandins C and E, see: Schnermann, M. J.; Beaudry, C. M.; Genung, N. E.; Canham, S. M.; Untiedt, N. L.; Karanikolas, B. D. W.; Sütterlin, C.; Overman, L. E. *J. Am. Chem. Soc.* **2011**, *133*, 17494–17503.
(23) Wang, H.; Kohler, P.; Overman, L. E.; Houk, K. N. *J. Am. Chem. Soc.* **2012**, *134*, 16054–16058.
(24) (a) Ruano, J. L. C.; Núñez, A., Jr.; Martín, M. R.; Fraile, A. *J. Org. Chem.* **2008***, 73*, 9366–9371. (b) Lu, X.; Zhang, C.; Xu, Z. *Acc. Chem. Res.* **2001**, *34*, 535–544.

(25) See the Supporting Information for a summary of the dihydroxylation conditions surveyed.
(26) These compounds were characterized by single-crystal X-ray analysis; X-ray coordinates were deposited with the Cambridge Crystallographic Data Centre: (a) **23**: CCDC1810845; (b) **37**: CCDC1447146; (c) **56**: CCDC1446028; (d) **57**: CCDC1446026; (e) **11**: CCDC1446027.
(27) For selected other examples of torsional effects governing stereoselectivities, see: (a) Caramella, P.; Rondan, N. G.; Paddon, M. N.; Houk, K. N. *J. Am. Chem. Soc.* **1981**, *103*, 2438–2440. (b) Rondan, N. G.; Paddon, M. N.; Caramella, P.; Mareda, J.; Mueller, P. H.; Houk, K. N. *J. Am. Chem. Soc.* **1982**, *104*, 4974–4976. (c) Paddon, M. N.; Rondan, N. G.; Houk, K. N. *J. Am. Chem. Soc.* **1982**, *104*, 7162–7166. (d) Houk, K. N.; Paddon, M. N.; Rondan, N. G.; Wu, Y.-D.; Brown, F. K.; Spellmeyer, D. C.; Metz, J. T.; Li, Y.; Loncharich, R. J. *Science* **1986**, *231*, 1108–1117. (e) Martinelli, M. J.; Peterson, B. C.; Khau, V. V.; Hutchinson, D. R.; Leanna, M. R.; Audia, J. E.; Droste, J. J.; Wu, Y.-D.; Houk, K. N. *J. Org. Chem.* **1994**, *59*, 2204–2210. (f) Lucero, M. J.; Houk, K. N. *J. Org. Chem.* **1998**, *63*, 6973–6977. (g) Cheong, P. H.; Yun, H.; Danishefsky, S. J.; Houk, K. N. *Org. Lett.* **2006**, *8*, 1513–1516.
(28) For selected recent reviews on radical reactions in organic synthesis, see: (a) Srikanth, G. S. C.; Castle, S. L. *Tetrahedron* **2005**, *61*, 10377–10441. (b) Rowlands, G. J. *Tetrahedron* **2009**, *65*, 8603–8655. (c) Rowlands, G. J. *Tetrahedron* **2010**, *66*, 1593–1636. (d) Yan, M.; Lo, J. C.; Edwards, J. T.; Baran, P. S. *J. Am. Chem. Soc.* **2016**, *138*, 12692–12714.
(29) For recent total syntheses examples in which a carbon radical bearing a $\beta$-alkoxy substituent was involved, see: (a) Nagatomo, M.; Koshimizu, M.; Masuda, K.; Tabuchi, T.; Urabe, D.; Inoue, M. *J. Am. Chem. Soc.* **2014**, *136*, 5916–5919. (b) Mukai, K.; Kasuaya, S.; Nakagawa, Y.; Urabe, D.; Inoue, M. *Chem. Sci.* **2015**, *6*, 3383–3387. (c) Fujino, H.; Nagatomo, M.; Paudel, A.; Panthee, S.; Hamamoto, H.; Sekimizu, K.;

Inoue, M. *Angew. Chem., Int. Ed.* **2017**, *56*, 11865–11869. (d) Kawamata, T.; Nagatomo, M.; Inoue, M. *J. Am. Chem. Soc.* **2017**, *139*, 1814–1817. (e) Edwards, J. T.; Merchant. R. R.; McClymont, K. S.; Knouse, K. W.; Qin, T.; Malins, L. R.; Vokits, B.; Shaw, S. A.; Bao, D. H.; Wei, F. L.; Zhou, T.; Eastgate, M. D.; Baran, P. S. *Nature* **2017**, *545*, 213–218. (f) Hashimoto, S.; Katoh, S.-I.; Kato, T.; Urabe, D.; Inoue, M. *J. Am. Chem. Soc.* **2017**, *139*, 16420−16429.
(30) (a) van Der Deen, H.; van Oeveren, A.; Kellogg, R. M.; Feringa, B. L. *Tetrahedron Lett.* **1999**, *40*, 1755–1758. (b) Moradei, O. M.; Paquette, L. A. *Org. Synth.* **2003**, *80*, 66−74. (c) Highly enantioenriched samples of both the (*R*)- and (*S*)-enantiomers 5-methoxy- and 5-menthoxybutenolides can be purchased from Accel Pharmtech or Proactive Molecular Research.
(31) (a) Brady, T. P.; Kim, S. H.; Wen, K.; Theodorakis, E. A. *Angew. Chem., Int. Ed.* **2004**, *43*, 739–742. (b) Granger, K.; Snapper, M. L. *Eur. J. Org. Chem.* **2012**, *12*, 2308–2311. (c) Alvarez-Manzaneda, E.; Chahboun, R.; Barranco, I.; Cabrera, E.; Alvarez, E.; Lara, A.; Alvarez-Manzaneda, R.; Hmamouchi, M.; Es-Samti, H. *Tetrahedron* **2007**, *63*, 11943–11951.
(32) Crich, D.; Hao, X. *J. Org. Chem.* **1999**, *64*, 4016–4024.
(33) Giese, B. *Angew. Chem., Int. Ed. Engl.* **1983**, *22*, 753–764.
(34) For selected recent total synthesis using Giese reactions to accomplish intermolecular fragment couplings, see: references 2b, 3a, (a) Ling, T.; Poupon, E.; Rueden, E. J.; Kim, S. H.; Theodorakis, E. A. *J. Am. Chem. Soc.* **2002**, *124*, 12261–12267. (b) Schnermann, M. J.; Overman, L. E. *Angew. Chem., Int. Ed.* **2012**, *51*, 9576–9580. (c) Sun, Y.; Li, R.; Zhang, W.; Li, A. *Angew. Chem., Int. Ed.* **2013**, *52*, 9201–9204. (d) Wang, L.; Wang, H.; Li, Y.; Tang, P. *Angew. Chem., Int. Ed.* **2015**, *54*, 5732–5735. (e) Müller, D. S.; Untiedt, N. L.; Dieskau, A. P.; Lackner, G. L.; Overman, L. E. *J. Am. Chem. Soc.* **2015**, *137*, 660–663. (f) Slutskyy, Y.; Jamison, C. R.; Lackner, G. L.; Müller, D. S.; Dieskau, A. P.; Untiedt, N. L.; Overman, L. E. *J. Org. Chem.* **2016**, *81*, 7029–7035. (g) Garnsey, M. R.; Slutskyy, Y.; Jamison, C. R.; Zhao, P.; Lee, J.; Rhee, Y. H.; Overman, L. E. *J. Org. Chem.* **2017**, DOI: 10.1021/acs.joc.7b02458.
(35) Lackner, G. L.; Quasdorf, K. W.; Overman, L. E. *J. Am. Chem. Soc.* **2013**, *135*, 15342–15345.
(36) (a) Gerster, M.; Renaud, P. *Synthesis* **1997**, *1997*, 1261–1267. (b) Yamada, K.; Yamamoto, Y.; Maekawa, M.; Tomioka, K. *J. Org. Chem.* **2004**, *69*, 1531–1534.

(37) See Supporting Information for details.

(38) (a) Thompson, D. K.; Hubert, C. N.; Wightman, R. H. *Tetrahedron* **1993**, *49*, 3827–3840. (b) Kim, H.-J.; Ricardo, A.; Illangkoon, H. I.; Kim, M. J.; Carrigan, M. A.; Frye, F.; Benner, S. A. *J. Am. Chem. Soc.* **2011**, *133*, 9457–9468.
(39) Pratsch, G.; Lackner, G. L.; Overman, L. E. *J. Org. Chem.* **2015**, *80*, 6025–6036.
(40) Okada, K.; Okamoto, K.; Morita, N.; Okubo, K.; Oda, M. *J. Am. Chem. Soc.* **1991**, *113*, 9401–9402.
(41) Tao, D. J.; Muuronen, M.; Slutskyy, Y.; Le, A.; Furche, F.; Overman, L. E. *Chem.-Eur. J.* **2016**, *22*, 8786–8790.
(42) For reviews on polyene cyclizations, see: (a) Yoder, R. A.; Johnston, J. N. *Chem. Rev.* **2005**, *105*, 4730–4756. (b) Ungarean, C. N.; Southgate, E. H.; Sarlah, D. *Org. Biomol. Chem.,* **2016**, *14*, 5454–5467.
(43) (a) Ishihara, K.; Nakamura, S.; Yamamoto, H. *J. Am. Chem. Soc.* **1999**, *121*, 4906–4907. (b) Ishihara, K.; Ishibashi, H.; Yamamoto, H. *J. Am. Chem. Soc.* **2002**, *124*, 3647–3655. (c) Ishibashi, H.; Ishihara, K.; Yamamoto, H. *J. Am. Chem. Soc.* **2004**, *126*, 11122–11123. (d) Ishihara, K.; Ishibashi, H.; Yamamoto, H. *J. Am. Chem. Soc.* **2001**, *123*, 1505–1506.
(44) (a) Surendra, K.; Corey, E. J. *J. Am. Chem. Soc.* **2012**, *134*, 11992–11994. (b) Surendra, K.; Rajendar, G.; Corey, E. J. *J. Am. Chem. Soc.* **2014**, *136*, 642–645.
(45) For early examples of forming *trans*-bicyclo[4.3.0]nonanes by polyene cyclization, see: (a) Gravestock, M. B.; Johnson, W. S.; Myers, R. F.; Bryson, T. A.; Miles, D. H.; Ratcliffe, B. E. *J. Am. Chem. Soc.* **1978**, *100*, 4268–4273. (b) Johnson, W. S.; Ward, C. E.; Boots, S. G.; Gravestock, M. B.; Markezich, R. L.; McCarry, B. E.; Okorie, D. A.; Parry, R. J. *J. Am. Chem. Soc.* **1981**, *103*, 88–98.
(46) (a) Johnson, W. S.; Gravestock, M. B.; McCarry, B. E. *J. Am. Chem. Soc.* **1971**, *93*, 4332–4334. (b) Guay, D.; Johnson, W. S.; Schubert, U. *J. Org. Chem.* **1989**, *54*, 4731–4732.
(47) $^{1}$H NMR analysis of the crude reaction mixture showed multiple polyene byproducts that are believed to be the result of undesired protonation of the propargylic silane in preference to the terminal alkene.
(48) *Trans*-hydrindane with an angular methyl substituent is ~2 kcal/mol higher in energy than the corresponding *cis* isomer, see: Gordon, H. L.; Freeman, S.; Hudlicky, T. *Synlett* **2005**, 2911–2914.
(49) (a) Mandai, T.; Matsumoto, T.; Kawada, M.; Tsuji, J. *J. Org. Chem.* **1992**, *57*, 1326–1327. (b) Mandai, T.; Matsumoto, T.; Kawada, M.; Tsuji, J. *Tetrahedron* **1993**, *49*, 5483–5493. (c) Tsuji, J.; Mandai, T. *Synthesis* **1996**, *1996*, 1–24.
(50) (a) Eder, U.; Sauer, G.; Wiechert, R. *Angew. Chem., Int. Ed. Engl.* **1971**, *10*, 496–497. (b) Enantiopure samples of (*S*)-enantiomer can be purchased from Apollo Scientific.
(51) Shigehisa, H.; Mizutani, T.; Tosaki, S.-Y.; Ohshima, T.; Shibasaki, M. *Tetrahedron* **2005**, *61*, 5057–5065.
(52) Myers, A. G.; Zheng, B. *Tetrahedron Lett.* **1996**, *37*, 4841–4844.
(53) (a) Miayano, S.; Yamashita, J.; Hashimoto, H. *Bull Chem. Soc. Jpn.* **1972**, *45*, 1946. (b) Denmark, S. E.; Edwards, J. P. *J. Org. Chem.* **1991**, *56*, 6974–6981.
(54) (a) Woodworth, C. W.; Buss, V.; Schleyer, P. V. R. *Chem. Commun.* **1968**, 569–570. (b) Simmons, H. E.; Cairns, T. L.; Vladuchick, S. A.; Hoiness, C. M. *Organic Reactions* **1973**, *20*, 1–131.
(55) Barton, D. H. R.; Bashiardes, G.; Pourrey, J.-L. *Tetrahedron Lett.* **1983**, *24*, 1605–1608.
(56) For pioneering work by Seebach on desymmetrizing alkylations of tartrate-based nucleophiles, see Naef, R.; Seebach, D.; *Angew. Chem., Int. Ed.* **1981**, *20*, 1030–1031.
(57) For pioneering work by Evans on desymmetrizing aldol reactions with tartrate-based nucleophiles, see: (a) Evans, D. A.; Barrow, J. C.; Leighton, J. L.; Robichaud, A. J. *J. Am. Chem. Soc.* **1994**, *116*, 12111–12112. (c) Evans, D. A.; Trotter, W.; Barrow, J. C. *Tetrahedron* **1997**, *53*, 8779–8794.
(58) Dess, D. B.; Martin, J. C. *J. Org. Chem.* **1983**, *48*, 4155–4156.
(59) Rapid decomposition of the aldehyde was observed within 24 h upon storage under vacuum or in –20 ºC freezer.
(60) For reviews, see: (a) Fürstner, A. *Chem. Rev.* **1999**, *99*, 991–1046. (b) Wessjohann, L. A.; Scheid, G. *Synthesis* **1999**, *1999*, 1–36. (c) Takai, K. *Organic Reactions* **2004**, *64*, 253–626. (d) Gil, A.; Albericio, F.; Álvarez, M. *Chem. Rev.* **2017**, *117*, 8420–8446.

(61) Brady, T. P.; Wallace, E. K.; Kim, S. H.; Guizzunti, G.; Malhotra, V.; Theodorakis, E. A. *Bioorg. Med. Chem. Let.* **2004**, *14*, 5035–5039.
(62) (a) Wan, Z.-K.; Choi, H.-W.; Kang, F.-A.; Nakajima, K.; Demeke, D.; Kishi, Y. *Org. Lett.* **2002**, *4*, 4431–4434. (b) Guo, H.; Dong, C.-G.; Kim, D.-S.; Urabe, D.; Wang, J.; Kim, J. T.; Liu, X.; Sasaki, T.; Kishi, Y. *J. Am. Chem. Soc.* **2009**, *131*, 15387–15393.
(63) The structural assignment of **52** was verified by single-crystal X-ray diffraction analysis of the(*N*-acyloxy)phthalimide analogue **56**.[26c]
(64) For an example of using this approach on a similar *trans*-hydrindene framework, see: Takaku, H.; Miyamoto, Y.; Asami, S.; Shimazaki, M.; Yamada, S.; Yamamoto, K.; Udagawa, N.; DeLuca, H. F.; Shimizu, M. *Bioorg. Med. Chem.* **2008**, *16*, 1796–1815.
(65) For a recent review on applications of [3,3]-sigmatropic rearrangements in natural product synthesis, see: Ilardi, E. A.; Stivala, C. E.; Zakarian, A. *Chem. Soc. Rev*. **2009**, *38*, 3133–3148.
(66) Müller, P.; Siegfried, B. *Helv. Chim. Acta* **1974**, *57*, 987–994.
(67) (a) Ishiwata, A.; Ito, Y. *Synlett* **2003**, *9*, 1339–1343. (b) Nicolaou, K. C.; Estrada, A. A.; Zak, M.; Lee, S. H.; Safina, B. S. *Angew. Chem., Int. Ed.* **2005**, *44*, 1378–1382.
(68) Addition of KHMDS to a colorless solution of **56** at –78 ºC led to an immediate color change to red, indicating formation of phthalimide anion.
(69) Ireland, R. E.; Wrigley, T. I.; Young, W. G. *J. Am. Chem. Soc.* **1959**, *81*, 2818–2821.

(70) We have failed to isolate **60** in pure form.

(71) Dahanukar, V. H.; Rychnovsky, S. D. *J. Org. Chem.* **1996**, *61*, 8317–8320.
(72) (a) Tao, J.; Perdew, J. P.; Staroverov, V. N.; Scuseria, G. E. *Phys. Rev. Lett.* **2003**, *91*, 146401–146404. (b) Staroverov, V. N.; Scuseria, G. E.; Tao, J.; Perdew, J. P. J. *Chem. Phys.* **2003**, *119*, 12129−12137.
(73) Weigend, F.; Ahlrichs, R. *Phys. Chem. Chem. Phys.* **2005**, *7*, 3297–3305.
(74) (a) Grimmer, S.; Antony, J.; Ehrlich, S.; Krige, H. *J. Chem. Phys.* **2010**, *132*, 154104. (b) Grimmer, S.; Ehrlich, S.; Goerigk, L. *J. Comput. Chem.* **2011**, *32*, 1456–1465.
(75) For a detailed discussion of the computational methods utilized in the study, see the Supporting Information.

(76) As the chloride substituent could lower the reduction potential of the α-acyloxy radical intermediate and favor reactivity by the enolate pathway, we confirmed that formation of the ACF product having the C-8 configuration of (–)-chromodorolide B would also be favored by the enolate pathway, see Supporting Information, Figure S7.

(77) Use of an $\alpha$-bromobutenolide is also predicted to favor formation of the desired ACF product (Table 1). However, this prediction could not be verified experimentally because of decomposition of the bromide-containing butenolide upon irradiation with blue LEDs.
(78) Nguyen, J. D.; D'Amato, E. M.; Narayanam, J. M. R.; Stephenson, C. R. J. *Nat. Chem.* **2012**, *4*, 854–859.
(79) Uoyama, H.; Goushi, K.; Shizu, K.; Nomura, H.; Adachi, C. *Nature*, **2012**, *492*, 234–238.
(80) For initial application of 4CzIPN in photoredox catalysis, see: Zhang, J.; Luo, J. *ACS Catal.* **2016**, *6*, 873–877.
(81) For a scalable preparation of 4CzIPN, see: Patel, N. P.; Kelly, C. B.; Siegenfeld, A. P.; Molander, G. A. *ACS Catal.* **2017**, *7*, 1766–1770.
(82) Barhoumi-Slimi, T. M.; Ben Diah, M. T.; Nsangou, M.;
El Gaied, M. M.; Khaddar, M. R. *J. Struc. Chem.* **2010**, *51*, 251–257.

(83) Use of other transfer hydrogenation reagents such as 1,4-cyclohexadiene or ammonium formate did not result in debenzylation of **71**.

Insert Table of Contents artwork here